

# Yukawas and trilinear Higgs terms from loops

Ulrich Haisch

*Rudolf Peierls Centre for Theoretical Physics, University of Oxford,  
OX1 3NP Oxford, United Kingdom*

It is illustrated how LHC precision measurements of rates and distributions in single-Higgs production can be used to constrain the charm Yukawa as well as the Higgs trilinear coupling.

## 1 Setting the stage

The interactions of the standard model (SM) Higgs boson are determined by the following Lagrangian density

$$\mathcal{L} \supset |D_\mu H|^2 - \sum_f (y_f \bar{f}_L H f_R + \text{h.c.}) - V, \quad V = -\mu |H|^2 + \lambda |H|^4, \quad (1)$$

where  $D_\mu$  is the  $SU(2)_L \times U(1)_Y$  covariant derivative,  $H$  is the Higgs doublet, the subscripts  $L, R$  denote the chirality of fermionic fields and  $y_f$  are the corresponding Yukawa couplings.

What do we know about the above interactions? From the ATLAS and CMS combination of the LHC Run I measurements of the Higgs boson production and decay rates,<sup>1</sup> it follows that the gauge-Higgs interactions, as encoded in the term  $|D_\mu H|^2$ , are at the level of  $\mathcal{O}(10\%)$  SM-like. The Yukawa interactions  $y_f \bar{f}_L H f_R + \text{h.c.}$ , on the other hand, have been tested with this accuracy only in the case of the tau lepton, while the constraints on the top and bottom Yukawa couplings just reach the  $\mathcal{O}(20\%)$  level. Apart from the muon Yukawa coupling which is marginally constrained by the combined ATLAS and CMS analysis, first and second generation Yukawa couplings are not directly probed at present. In the case of the Higgs potential  $V$ , we know the vacuum expectation value (VEV) of  $H$  for a long time, and the discovery of a spin-0 CP-even state of  $m_h \simeq 125 \text{ GeV}$  at the LHC tells us about the second derivative of  $V$  around its VEV, as this quantity determines the Higgs mass. The trilinear and quartic Higgs self-interactions that result from (1) are however essentially untested at the moment.

In the following it will be shown that LHC precision measurements of rates and distributions in single-Higgs production can be used to constrain some of the presently poorly known Higgs interactions terms appearing in (1). The two explicit examples that we will discuss in some detail are the charm Yukawa coupling and the Higgs trilinear coupling.

## 2 Charm Yukawa coupling

It has been common lore<sup>2</sup> that extractions of  $y_c$  can only be performed with a few-percent uncertainty at an  $e^+e^-$  machine such as the ILC.<sup>3</sup> Gaining direct access to  $y_c$  is however not hopeless, since in its high-luminosity run the LHC (HL-LHC) will produce around  $1.7 \cdot 10^8$  Higgses bosons per experiment with  $3 \text{ ab}^{-1}$  of integrated luminosity.<sup>4</sup> In fact, several different strategies have been proposed to constrain modifications  $\kappa_c = y_c/y_c^{\text{SM}}$ . A first way to probe  $\kappa_c$  consists in searching for the exclusive decay  $h \rightarrow J/\psi \gamma$ .<sup>5,6,7</sup> While reconstructing the  $J/\psi$  via its dimuon decay leads to a clean experimental signature, the small branching ratio of  $1.8 \cdot 10^{-7}$ , implies that only 30 signal events can be expected at each ATLAS and CMS. This makes a detection challenging given the large continuous background due to QCD production of charmonia and a jet faking a photon.<sup>8,9</sup> The process  $h \rightarrow c\bar{c}\gamma$  can also be used to bound  $\kappa_c$  and the constraining power has recently been found to be at least comparable to that of  $h \rightarrow J/\psi \gamma$ .<sup>10</sup> Strategies with larger signal cross sections are  $pp \rightarrow V c\bar{c}$  where  $V = W, Z$ ,<sup>9,11</sup> the  $pp \rightarrow h c$ <sup>12</sup> channel and  $gg \rightarrow h \rightarrow c\bar{c}$ .<sup>13</sup> These searches rely on charm tagging ( $c$ -tagging). Since  $c$ -tagging algorithms at ATLAS and CMS are currently inefficient, bottom jets cannot be discriminated perfectly from

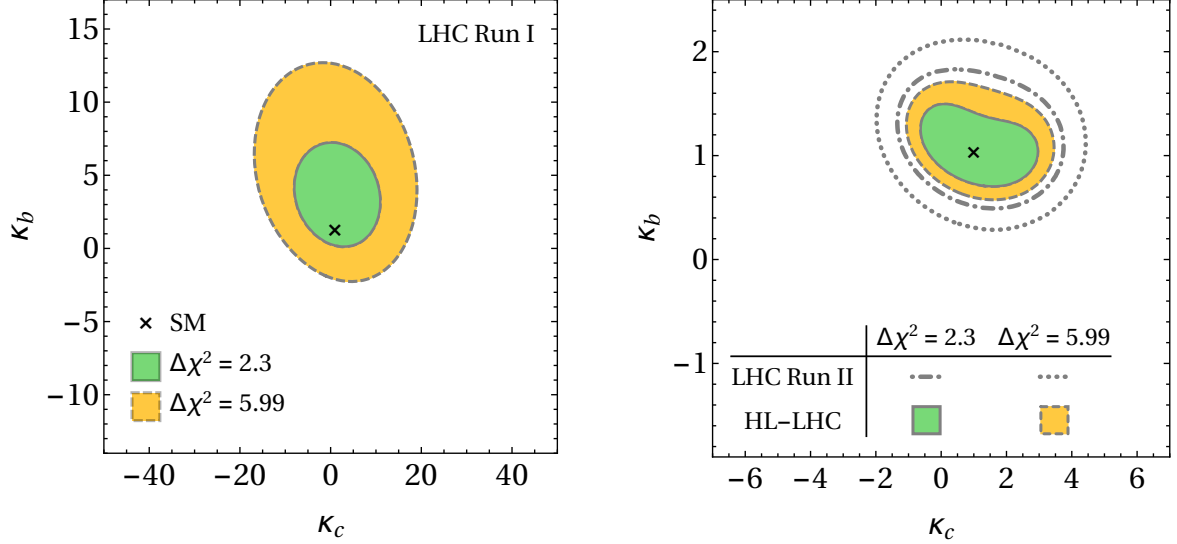


Figure 1 – Left: The  $\Delta\chi^2 = 2.3$  and  $\Delta\chi^2 = 5.99$  regions in the  $\kappa_c$ - $\kappa_b$  plane following from the combination of the ATLAS measurements of the normalised  $p_{T,h}$  distribution in the  $h \rightarrow \gamma\gamma$  and  $h \rightarrow ZZ^* \rightarrow 4\ell$  channels. The SM point is indicated by the black cross. Right: Projected future constraints in the  $\kappa_c$ - $\kappa_b$  plane. The figure shows projections for the LHC Run II (HL-LHC) with  $0.3 \text{ ab}^{-1}$  ( $3 \text{ ab}^{-1}$ ) of integrated luminosity at  $\sqrt{s} = 13 \text{ TeV}$ .

charm jets so that the latter modes not only measure  $\kappa_c$ , but certain linear combinations of  $\kappa_c$  and  $\kappa_b = y_b/y_b^{\text{SM}}$ . Notice that despite its lower acceptance in pseudorapidity, LHCb has recently also obtained a first limit on  $pp \rightarrow Vc\bar{c}$ ,<sup>14</sup> and hence in the long run might be able to set relevant bounds on the modification  $\kappa_c$  as well.

Another independent procedure to constrain  $\kappa_c$ ,<sup>16</sup> that does not suffer one of the aforementioned limitations, is based on the observation that the cross section in gluon-fusion Higgs production provides sensitivity to  $\kappa_t = y_t/y_t^{\text{SM}}$  and  $\kappa_b$  through the interference of top and bottom loops<sup>1</sup>

$$\sigma(gg \rightarrow h) \propto 1.06\kappa_t^2 + 0.01\kappa_b^2 - 0.07\kappa_t\kappa_b. \quad (2)$$

Such interference effects appear not only in the total rate, but in all  $gg \rightarrow hj$  distributions such as the transverse momentum  $p_{T,h}$  of the Higgs boson. In fact, these contributions are dynamically enhanced by logarithms<sup>15</sup> of the form  $\kappa_Q m_Q^2/m_h^2 \ln^2(p_{T,h}^2/m_Q^2)$  with  $Q = b, c$ . If instead the Higgs is produced in  $gQ \rightarrow hQ$ ,  $Q\bar{Q} \rightarrow hg$ , the resulting leading order (LO) differential cross section scales as  $\kappa_Q^2$ , with an additional suppression factor of  $\mathcal{O}(\alpha_s/\pi)$  for each initial-state sea-quark parton distribution function which is generated from gluon splitting. Due to the different Lorentz structure of the amplitudes in the  $m_Q \rightarrow 0$  limit, the  $gg \rightarrow hj$  and  $gQ \rightarrow hQ$ ,  $Q\bar{Q} \rightarrow hg$  processes do not interfere at  $\mathcal{O}(\alpha_s^2)$ . This ensures that no terms scaling linearly in  $\kappa_Q$  are present in the  $gQ \rightarrow hQ$ ,  $Q\bar{Q} \rightarrow hg$  channels at this order.

Since the gluon-fusion and quark-initiated processes lead to different  $p_{T,h}$  distributions, the two Higgs production mechanism can be experimentally disentangled. This feature has been exploited to set constraints on  $y_{b,c,s}$ <sup>16</sup> as well as  $y_{u,d}$ .<sup>17</sup> In particular, it has been shown that in the case of the bottom and charm Yukawa couplings both the effects linear and quadratic in  $\kappa_{b,c}$  can be phenomenologically relevant, while in the case of the light quarks only terms proportional to  $\kappa_{s,u,d}^2$  matter. Since the deviations of the  $p_{T,h}$  spectrum amount to only several percent for  $\mathcal{O}(1)$  modifications of  $\kappa_{b,c}$  (as expected from (2)), precise theoretical predictions for the  $gg \rightarrow hj$  and  $gQ \rightarrow hQ$ ,  $Q\bar{Q} \rightarrow hg$  channels are needed to derive faithful bounds on the bottom and charm Yukawa couplings. In the case of  $gg \rightarrow hj$ , next-to-leading order (NLO) corrections to the spectrum in the Higgs effective field theory (HEFT)<sup>18,19,20</sup> are included using MCFM.<sup>21</sup> The total cross sections for inclusive Higgs production are obtained from HIGLU,<sup>22</sup> taking into account the next-to-next-to-leading order (NNLO) corrections in the HEFT.<sup>23,24,25</sup> Sudakov logarithms

Method	LHC Run I	LHC Run II	HL-LHC
$h \rightarrow J/\psi\gamma$ <sup>7,9</sup>	$ \kappa_c  < 429$	$ \kappa_c  \lesssim 80$	$ \kappa_c  \lesssim 45$
$h \rightarrow c\bar{c}\gamma$ <sup>10</sup>	—	—	$ \kappa_c  < 6.3$
$pp \rightarrow Vc\bar{c}$ <sup>9</sup>	$ \kappa_c  < 234$	$ \kappa_c  < 21$	$ \kappa_c  < 3.7$
$pp \rightarrow hc$ <sup>12</sup>	—	—	$ \kappa_c  < 2.6$
$p_{T,h}$ spectrum <sup>16</sup>	$\kappa_c \in [-16, 18]$	$\kappa_c \in [-1.4, 3.8]$	$\kappa_c \in [-0.6, 3.0]$

Table 1: Sensitivities for probing the modification  $\kappa_c$  of the charm Yukawa coupling with various methods. The 95% CL bounds as quoted in the literature after LHC Run I and II as well as the HL-LHC phase are given.

of the form  $\ln(p_{T,h}/m_h)$  are resummed up to next-to-next-to-leading logarithmic order.<sup>26,27,28</sup> The  $gQ \rightarrow hQ$ ,  $Q\bar{Q} \rightarrow hg$  contributions to the  $p_{T,h}$  distribution are calculated at NLO with **MG5aMC@NLO**.<sup>29</sup> The theoretical uncertainties obtained in this way amount to around  $\pm 5\%$ <sup>16</sup> and could be improved by taking into account recent theoretical developments in  $gg \rightarrow hj$ <sup>30,31,32</sup> and  $gQ \rightarrow hQ$ ,  $Q\bar{Q} \rightarrow hg$ .<sup>33</sup> Since non-perturbative corrections to the  $p_{T,h}$  distribution are not larger than  $\pm 2\%$  in the region of moderate  $p_{T,h}$ ,<sup>16,34</sup> the theoretical predictions can be expected to reach an accuracy of a few percent in the not too far future.

In order to derive the current constraints on  $\kappa_b$  and  $\kappa_c$ , we harness the normalised  $p_{T,h}$  distribution in inclusive Higgs production.<sup>35</sup> This spectrum is obtained by ATLAS from a combination of  $h \rightarrow \gamma\gamma$  and  $h \rightarrow ZZ^* \rightarrow 4\ell$  decays and based on  $20.3\text{ fb}^{-1}$  of  $\sqrt{s} = 8\text{ TeV}$  data. In our analysis, we include the first seven bins in the range  $p_{T,h} \in [0, 100]\text{ GeV}$  whose experimental uncertainty is dominated by the statistical error. In the left panel of Figure 1 the  $\Delta\chi^2 = 2.3$  and  $\Delta\chi^2 = 5.99$  contours (corresponding to a 68% and 95% confidence level (CL) for a Gaussian distribution) in the  $\kappa_c$ - $\kappa_b$  plane are displayed. By profiling over  $\kappa_b$ , one obtains the following 95% CL bound on  $\kappa_c$ <sup>16</sup>

$$\kappa_c \in [-16, 18], \quad (\text{LHC Run I}). \quad (3)$$

As can be seen from Table 1, this limit is significantly stronger than the existing bounds on the charm Yukawa coupling from  $h \rightarrow J/\psi\gamma$  and  $pp \rightarrow Vc\bar{c}$ . It is also more stringent than the limit  $|\kappa_c| \lesssim 130$  following from the measurements of the total Higgs width, but it is not competitive with the bound  $|\kappa_c| \lesssim 6.2$  that derives from a global analysis of LHC Run I Higgs data.<sup>11</sup>

We study two benchmark cases to demonstrate the LHC prospects of extracting  $\kappa_c$  through analyses of the  $p_{T,h}$  spectrum. Our LHC Run II scenario employs  $0.3\text{ ab}^{-1}$  of integrated luminosity and assumes a systematic error of  $\pm 3\%$  on the experimental side and a total theoretical uncertainty of  $\pm 5\%$ . This means that we envision that the non-statistical uncertainties present at LHC Run I can be halved in the coming years, which seems plausible. Our HL-LHC scenario instead uses  $3\text{ ab}^{-1}$  of data and foresees a reduction of both systematic and theoretical errors by another factor of two, leading to uncertainties of  $\pm 1.5\%$  and  $\pm 2.5\%$ , respectively. We stress that this last scenario is illustrative of the reach that can be achieved with improved theory uncertainties. The corresponding fit results are presented on the right-hand side in Figure 1. The unshaded contours refer to the LHC Run II scenario with the dot-dashed (dotted) lines corresponding to  $\Delta\chi^2 = 2.3$  (5.99). Analogously, the shaded contours with the solid (dashed) lines refer to the HL-LHC. By profiling over  $\kappa_b$ , one finds in the LHC Run II scenario the following 95% CL bound on the  $y_c$  modifications<sup>16</sup>

$$\kappa_c \in [-1.4, 3.8], \quad (\text{LHC Run II}), \quad (4)$$

while the corresponding HL-LHC bound reads<sup>16</sup>

$$\kappa_c \in [-0.6, 3.0], \quad (\text{HL-LHC}). \quad (5)$$

As is evident from Table 1, these limits compare well not only with the projected reach of other proposed strategies but also have the nice feature that they are controlled by the systematic

uncertainties that can be reached in the future. This is not the case for extractions of  $y_c$  using the  $h \rightarrow J/\psi\gamma$ ,  $h \rightarrow c\bar{c}\gamma$ ,  $pp \rightarrow Vc\bar{c}$  and  $pp \rightarrow hc$  channels, which are either limited by small signal-to-background ratios or by the charm-bottom discrimination of heavy-flavour tagging.

### 3 Trilinear Higgs coupling

After electroweak (EW) symmetry breaking the self-interactions of the Higgs field  $h$  in the SM can be parameterised by

$$V \supset \lambda v h^3 + \frac{\chi}{4} h^4, \quad \lambda = \chi = \frac{m_h^2}{2v^2}, \quad (6)$$

One way to experimentally constrain the coefficients  $\lambda$  and  $\chi$  consists in measuring double-Higgs and triple-Higgs production. Since the cross section for  $pp \rightarrow 3h$  production is of  $\mathcal{O}(0.1 \text{ fb})$  at  $\sqrt{s} = 14 \text{ TeV}$  even the HL-LHC will only allow to set very loose bounds on the Higgs quartic. The prospects to observe double-Higgs production at the HL-LHC is considerably better because the  $pp \rightarrow hh$  cross section amounts to  $\mathcal{O}(33 \text{ fb})$  at the same centre-of-mass energy. Measuring double-Higgs production at the HL-LHC however still remains challenging and as a result even with the full data set of  $3 \text{ ab}^{-1}$  only an  $\mathcal{O}(1)$  determination of the trilinear Higgs coupling  $\lambda$  seems possible under optimistic assumptions.

The coefficient  $\lambda$  is however also subject to indirect constraints from processes such as single-Higgs production<sup>36,37,38,39</sup> or EW precision observables<sup>40,41</sup> since a modified  $h^3$  coupling alters these observables at the loop level. In order to describe modifications of the trilinear Higgs coupling in a model-independent fashion, one can employ the SM effective field theory and add dimension-six operators to the SM Lagrangian density

$$\mathcal{L}^{(6)} = \sum_k \frac{\bar{c}_k}{v^2} O_k, \quad O_6 = -\lambda |H|^6, \quad (7)$$

where  $v \simeq 246 \text{ GeV}$  denotes the Higgs VEV. Under the assumption that the operator  $O_6$  represents the only relevant modification of the Higgs self-interactions at tree level, instead of the result (6) one then finds

$$V \supset \kappa_\lambda \lambda v h^3 + \kappa_\chi \frac{\chi}{4} h^4, \quad \kappa_\lambda = 1 + \bar{c}_6, \quad \kappa_\chi = 1 + 6\bar{c}_6. \quad (8)$$

These relations allow one to parameterise a modified trilinear Higgs coupling via the Wilson coefficient  $\bar{c}_6 = \kappa_\lambda - 1$  or equivalent  $\kappa_\lambda$ . Other operators such as  $O_H = (\partial_\mu |H|^2)^2$  or  $O_8 = |H|^8$  also change the  $h^3$  coupling at tree level, but will not be discussed in what follows.

The operator  $O_6$  introduced in (7) modifies vector boson fusion (VBF), associated  $Vh$ <sup>38,39</sup> as well as  $t\bar{t}h$  production<sup>38</sup> at the one-loop level, while it enters the gluon-fusion channel at two loops.<sup>37,38</sup> Higgs decays to fermions,  $W$  and  $Z$  pairs are altered at one loop,<sup>38,39</sup> while modifications of the digluon and diphoton rates are again a two-loop effect.<sup>37,38</sup> All production and decay channels receive two types of contributions: firstly, a process dependent one, which is linear in  $\bar{c}_6$  and secondly, a universal one associated to the Higgs wave function renormalisation, which contains a piece quadratic in  $\bar{c}_6$ . In order to give an impression of the complexity of the corresponding perturbative calculations, let us quote an explicit expression for the non-universal part of the two-loop  $gg \rightarrow h$  form factor. Performing an asymptotic expansion in the ratio  $r = m_h^2/m_t^2$ , one finds that the sought contribution is proportional to<sup>42</sup>

$$\begin{aligned} & \ln r + \frac{\pi}{\sqrt{3}} - \frac{23}{12} + r \left( \frac{7}{10} \ln r + \frac{7\pi}{20\sqrt{3}} - \frac{259}{240} \right) + r^2 \left( \frac{349}{1008} \ln r + \frac{23\pi}{240\sqrt{3}} - \frac{464419}{1058400} \right) \\ & + r^3 \left( \frac{1741}{10800} \ln r + \frac{13\pi}{525\sqrt{3}} - \frac{31795373}{190512000} \right) + r^4 \left( \frac{10817}{138600} \ln r + \frac{1789\pi}{277200\sqrt{3}} - \frac{40370773}{614718720} \right) \\ & + r^5 \left( \frac{2798759}{68796000} \ln r + \frac{439357\pi}{252252000\sqrt{3}} - \frac{2551088981767}{90901530720000} \right) + \mathcal{O}(r^6), \end{aligned} \quad (9)$$

where the terms up to order  $r^3$  have already been given before,<sup>38</sup> while the  $r^4$  and  $r^5$  terms are presented here for the first time.

So how do the direct and indirect limits on  $\kappa_\lambda$  compare after LHC Run I, if only the trilinear Higgs coupling is allowed to deviate from the SM? Performing a  $\chi^2$  fit with  $\Delta\chi^2 = 3.84$  corresponding to a 95% CL for a Gaussian distribution, one obtains from double-Higgs production<sup>37</sup>

$$\kappa_\lambda \in [-14.5, 19.1], \quad (pp \rightarrow hh \text{ at LHC Run I}), \quad (10)$$

while the combination of the LHC Run I single-Higgs data<sup>1</sup> leads to

$$\kappa_\lambda \in [-7.7, 15.1], \quad (pp \rightarrow h \text{ at LHC Run I}). \quad (11)$$

The quoted limit from  $pp \rightarrow h$  compares well with other existing single-Higgs extractions<sup>37,38,39</sup> and is slightly more stringent than (10) as well as the bound that can be derived from EW precision observables.<sup>40,41</sup> It has been derived by combining the results for LO gluon-fusion<sup>38,42</sup> and NNLO VBF and  $Vh$  production<sup>39</sup> with that of LO  $t\bar{t}h$  production.<sup>38</sup>

The results (10) and (11) indicate that to exploit the full LHC potential all available informations on the  $h^3$  term should be combined. Most of the existing studies of indirect constraints on the trilinear Higgs coupling are based on the simplified assumption that only the  $h^3$  vertex is modified while all other Higgs interactions remain SM-like. Recently<sup>43</sup> this assumption has been dropped and ten parameter fits allowing for modifications  $\kappa_\lambda$  have been performed. In this way it has been shown that standard global Higgs analyses suffer from degeneracies that prevent one from extracting robust bounds on each individual coupling (or Wilson coefficient) once large non-standard  $h^3$  interactions are considered. The inclusion of  $pp \rightarrow hh$  production as well as the use of differential measurements in the associated single-Higgs production channels  $Vh$  and  $t\bar{t}h$ , can however help to overcome the limitations of a global Higgs-coupling fit. Including differential information on both single-Higgs and double-Higgs production, one finds from the ten parameter fit the following 95% CL limit<sup>43</sup>

$$\kappa_\lambda \in [-0.7, 7.1], \quad (pp \rightarrow h \text{ and } pp \rightarrow hh \text{ differential at HL-LHC}), \quad (12)$$

assuming an integrated luminosity of  $3 \text{ ab}^{-1}$ . To which extent the result (12) represents the ultimate limit on  $\kappa_\lambda$  that can be obtained at the HL-LHC requires further study, in particular a detailed assessment of the experimental uncertainties entering the global  $\chi^2$  analysis.

In order to further illustrate the importance to measure differential Higgs distributions and to include them into global analyses of Higgs couplings, we consider besides (7) the following three dimension-six operators

$$\begin{aligned} O_{HW} &= \frac{8i}{g} (D_\mu H^\dagger \tau^i D_\nu H) W^{i,\mu\nu}, \\ O_W &= \frac{4i}{g} (H^\dagger \tau^i \overleftrightarrow{D}_\mu H) D_\nu W^{i,\mu\nu}, \\ O_B &= \frac{2ig'}{g} (H^\dagger \overleftrightarrow{D}_\mu H) D_\nu B^{\mu\nu}, \end{aligned} \quad (13)$$

which unlike  $O_6$  modify the  $VVh$  vertex at tree level. In (13) the variables  $g$  and  $g'$  denote the  $SU(2)_L$  and  $U(1)_Y$  gauge coupling, respectively,  $W^{i,\mu\nu}$  and  $B^{\mu\nu}$  are the corresponding field-strength tensors, the derivative operator  $\overleftrightarrow{D}_\mu$  is defined as  $H^\dagger \overleftrightarrow{D}_\mu H = H^\dagger D_\mu H - (D_\mu H^\dagger) H$  and  $\tau^i = \sigma^i/2$  with  $\sigma^i$  the usual Pauli matrices.

On the left in Figure 2, we show the  $p_{T,h}$  distribution in  $Wh$  production at  $\sqrt{s} = 13 \text{ TeV}$  normalised to the SM prediction for three different sets of Wilson coefficients.<sup>44</sup> In the case of  $\bar{c}_{HW} = 0.03$  (blue), one observes a sizeable enhancement in the tail of the  $p_{T,h}$  spectrum that

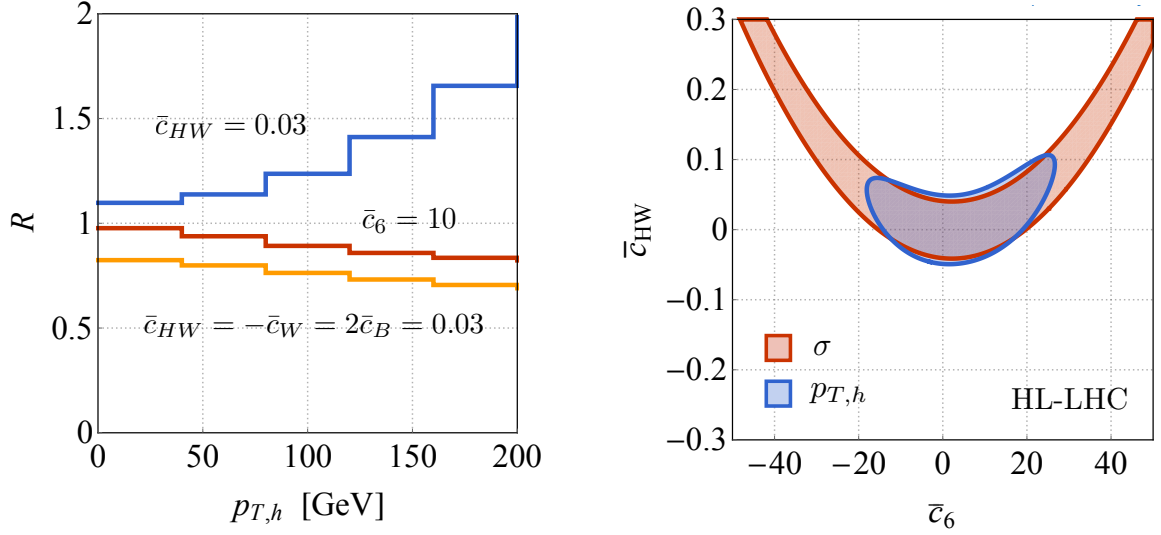


Figure 2 – Left: The  $p_{T,h}$  distributions in  $Wh$  production normalised to the SM spectrum at  $\sqrt{s} = 13$  TeV. The coloured curves correspond to different choices of Wilson coefficients. The coefficients  $\bar{c}_k$  not indicated in the plot are set to zero. Right: Constraints at 95% CL in the  $\bar{c}_6 - \bar{c}_{HW}$  plane that follow from a hypothetical measurement of the  $Wh$  channel at the HL-LHC. The red contour is obtained by a fit to the inclusive cross section, while the blue region derives from a shape-fit to the  $p_{T,h}$  distribution.

amounts to around 50% at  $p_{T,h} \simeq 150$  GeV, while for the choice  $\bar{c}_{HW} = -\bar{c}_W = 2\bar{c}_B = 0.03$  (orange) the event rate is reduced by about  $-15\%$  with respect to the SM, almost independently of the precise  $p_{T,h}$  value. The qualitatively different behaviour of the two  $p_{T,h}$  distributions can be understood by noticing that the leading  $p_{T,h}^2$  dependence of  $d\sigma/dp_{T,h}$  is proportional to the combination  $\bar{c}_{HW} + \bar{c}_W$  of Wilson coefficients which is non-zero for the former but zero for the latter choice. In the case of  $\bar{c}_6 = 10$  (red), one finally sees that the deviations in the  $p_{T,h}$  spectrum change approximately linearly with  $p_{T,h}$  and reach roughly  $-10\%$  at  $p_{T,h} \simeq 150$  GeV.

The observed shape differences can be used to better constrain the above benchmark cases compared to a fit that employs the information on the corresponding inclusive measurement only. This feature is illustrated in the right panel of Figure 2, which displays the 95% CL regions in the  $\bar{c}_6 - \bar{c}_{HW}$  plane that follow from a hypothetical HL-LHC measurement of the total cross section (red) and the  $p_{T,h}$  spectrum (blue) in the  $Wh$  channel.<sup>44</sup> From the plot it is evident that the fit to the inclusive measurement has a flat direction that allows for large correlated effects in  $\bar{c}_6$  and  $\bar{c}_{HW}$ , while this degeneracy is resolved by the shape-fit to the  $p_{T,h}$  distribution. This simple example illustrates nicely that differential Higgs measurements can give important additional informations compared to standard Higgs-coupling fits.

#### 4 Final words

The overarching goal of this presentation was to emphasise that LHC precision measurements of rates and distributions in single-Higgs production can help to better constrain some of the Higgs interactions that are crudely known at present. The two examples that we have discussed in some detail were the charm Yukawa and the Higgs trilinear coupling. In both cases it is important to stress that to fully exploit the physics potential of the LHC one should try to combine all known search strategies. For the charm Yukawa coupling these are  $h \rightarrow J/\psi\gamma$ ,  $h \rightarrow c\bar{c}\gamma$ ,  $pp \rightarrow Vc\bar{c}$ ,  $pp \rightarrow hc$  as well as single-Higgs distributions, while for what concerns the trilinear Higgs coupling a combination of the constraints arising from  $pp \rightarrow hh$ ,  $pp \rightarrow h$  and the EW precision measurements seems essential. The importance of measurements of distributions in gluon-fusion Higgs,  $Vh$ , VBF and  $t\bar{t}h$  production cannot be overemphasised in this context, since differential information has been shown to greatly enhance the sensitivity to the structure



of the underlying theory. Such measurements should therefore be pursued with vigour by both the ATLAS and CMS collaborations in the future LHC runs.

## Acknowledgments

A big thank you to Fady Bishara, Wojtek Bizon, Martin Gorbahn, Pier Francesco Monni, Emanuele Re and Giulia Zanderighi for enjoyable collaborations on the topics discussed in this proceedings. I wish to thank the organisers of Recontres Moriond EW 2017 for the invitation to give this talk and I am grateful to many participant, in particular to Andre David, Stefano Di Vita, Giuliano Panico and Gavin Salam, for interesting discussions. The continued hospitality and support of the CERN Theoretical Physics Department is highly appreciated.

## References

1. G. Aad *et al.* [ATLAS and CMS Collaborations], JHEP **1608**, 045 (2016) [arXiv:1606.02266 [hep-ex]].
2. M. E. Peskin, arXiv:1207.2516 [hep-ph].
3. H. Ono and A. Miyamoto, Eur. Phys. J. C **73**, no. 3, 2343 (2013) [arXiv:1207.0300 [hep-ex]].
4. S. Dawson *et al.*, arXiv:1310.8361 [hep-ex].
5. G. T. Bodwin, F. Petriello, S. Stoynev and M. Velasco, Phys. Rev. D **88**, no. 5, 053003 (2013) [arXiv:1306.5770 [hep-ph]].
6. A. L. Kagan, G. Perez, F. Petriello, Y. Soreq, S. Stoynev and J. Zupan, Phys. Rev. Lett. **114**, no. 10, 101802 (2015) [arXiv:1406.1722 [hep-ph]].
7. M. König and M. Neubert, JHEP **1508**, 012 (2015) [arXiv:1505.03870 [hep-ph]].
8. G. Aad *et al.* [ATLAS Collaboration], Phys. Rev. Lett. **114**, no. 12, 121801 (2015) [arXiv:1501.03276 [hep-ex]].
9. G. Perez, Y. Soreq, E. Stamou and K. Tobioka, Phys. Rev. D **93**, no. 1, 013001 (2016) [arXiv:1505.06689 [hep-ph]].
10. T. Han and X. Wang, arXiv:1704.00790 [hep-ph].
11. G. Perez, Y. Soreq, E. Stamou and K. Tobioka, Phys. Rev. D **92**, no. 3, 033016 (2015) [arXiv:1503.00290 [hep-ph]].
12. I. Brivio, F. Goertz and G. Isidori, Phys. Rev. Lett. **115**, no. 21, 211801 (2015) [arXiv:1507.02916 [hep-ph]].
13. C. Delaunay, T. Golling, G. Perez and Y. Soreq, Phys. Rev. D **89**, no. 3, 033014 (2014) [arXiv:1310.7029 [hep-ph]].
14. LHCb collaboration, [LHCb-CONF-2016-006](#).
15. U. Baur and E. W. N. Glover, Nucl. Phys. B **339**, 38 (1990).
16. F. Bishara, U. Haisch, P. F. Monni and E. Re, Phys. Rev. Lett. **118**, no. 12, 121801 (2017) [arXiv:1606.09253 [hep-ph]].
17. Y. Soreq, H. X. Zhu and J. Zupan, JHEP **1612**, 045 (2016) [arXiv:1606.09621 [hep-ph]].
18. D. de Florian, M. Grazzini and Z. Kunszt, Phys. Rev. Lett. **82**, 5209 (1999) [hep-ph/9902483].
19. V. Ravindran, J. Smith and W. L. Van Neerven, Nucl. Phys. B **634**, 247 (2002) [hep-ph/0201114].
20. C. J. Glosser and C. R. Schmidt, JHEP **0212**, 016 (2002) [hep-ph/0209248].
21. J. M. Campbell, R. K. Ellis and W. T. Giele, Eur. Phys. J. C **75**, no. 6, 246 (2015) [arXiv:1503.06182 [physics.comp-ph]].
22. M. Spira, hep-ph/9510347.
23. R. V. Harlander and W. B. Kilgore, Phys. Rev. Lett. **88**, 201801 (2002) [hep-ph/0201206].
24. C. Anastasiou and K. Melnikov, Nucl. Phys. B **646**, 220 (2002) [hep-ph/0207004].

25. V. Ravindran, J. Smith and W. L. van Neerven, Nucl. Phys. B **665**, 325 (2003) [hep-ph/0302135].
26. G. Bozzi, S. Catani, D. de Florian and M. Grazzini, Phys. Lett. B **564**, 65 (2003) [hep-ph/0302104].
27. T. Becher and M. Neubert, Eur. Phys. J. C **71**, 1665 (2011) [arXiv:1007.4005 [hep-ph]].
28. P. F. Monni, E. Re and P. Torrielli, Phys. Rev. Lett. **116**, no. 24, 242001 (2016) [arXiv:1604.02191 [hep-ph]].
29. M. Wiesemann, R. Frederix, S. Frixione, V. Hirschi, F. Maltoni and P. Torrielli, JHEP **1502**, 132 (2015) [arXiv:1409.5301 [hep-ph]].
30. T. Becher, M. Neubert and L. Rothen, JHEP **1310**, 125 (2013) [arXiv:1307.0025 [hep-ph]].
31. K. Melnikov and A. Penin, JHEP **1605**, 172 (2016) [arXiv:1602.09020 [hep-ph]].
32. J. M. Lindert, K. Melnikov, L. Tancredi and C. Wever, Phys. Rev. Lett. **118**, no. 25, 252002 (2017) [arXiv:1703.03886 [hep-ph]].
33. R. V. Harlander, A. Tripathi and M. Wiesemann, Phys. Rev. D **90**, no. 1, 015017 (2014) [arXiv:1403.7196 [hep-ph]].
34. T. Becher, M. Neubert and D. Wilhelm, JHEP **1305**, 110 (2013) [arXiv:1212.2621 [hep-ph]].
35. G. Aad *et al.* [ATLAS Collaboration], Phys. Rev. Lett. **115**, no. 9, 091801 (2015) [arXiv:1504.05833 [hep-ex]].
36. M. McCullough, Phys. Rev. D **90**, no. 1, 015001 (2014) Erratum: [Phys. Rev. D **92**, no. 3, 039903 (2015)] [arXiv:1312.3322 [hep-ph]].
37. M. Gorbahn and U. Haisch, JHEP **1610**, 094 (2016) [arXiv:1607.03773 [hep-ph]].
38. G. Degrossi, P. P. Giardino, F. Maltoni and D. Pagani, JHEP **1612**, 080 (2016) [arXiv:1607.04251 [hep-ph]].
39. W. Bizon, M. Gorbahn, U. Haisch and G. Zanderighi, arXiv:1610.05771 [hep-ph].
40. G. Degrossi, M. Fedele and P. P. Giardino, JHEP **1704**, 155 (2017) [arXiv:1702.01737 [hep-ph]].
41. G. D. Kribs, A. Maier, H. Rzehak, M. Spannowsky and P. Waite, Phys. Rev. D **95**, no. 9, 093004 (2017) [arXiv:1702.07678 [hep-ph]].
42. M. Gorbahn and U. Haisch, in preparation.
43. S. Di Vita, C. Grojean, G. Panico, M. Riembau and T. Vantalon, arXiv:1704.01953 [hep-ph].
44. W. Bizon *et al.*, in preparation.